RSC Sustainability

ROYAL SOCIETY OF CHEMISTRY

PAPER

View Article Online
View Journal | View Issue

Cite this: *RSC Sustainability*, 2026, **4**, 477

Life-cycle analysis of microalgae-based polyurethane foams

Ulises R. Gracida-Alvarez, [a] Matthew R. Wiatrowski, [b] Pahola Thathiana Benavides, *[a] Jingyi Zhang, [a] Ryan Davis [b] and Troy R. Hawkins [a]

Polyurethane plastics are essential in many consumer and commercial products such as insulation, furniture, automotive interiors, and clothing. Pathways for producing polyurethane from microalgae offer an opportunity to reduce greenhouse gas emissions and other environmental impacts and can incorporate processes that avoid the use of toxic isocyanates typically used in conventional polyurethane production processes. In this study, the greenhouse gas emissions, fossil energy, and water consumption of biobased polyurethane and biobased non-isocyanate polyurethane were evaluated *via* life-cycle analysis using the R&D Greenhouse Gases, Regulated Emissions, and Energy Use in Technologies model. Microalgae-based polyurethane foam was found to achieve greenhouse gas emission reductions of up to 79% compared with conventional polyurethane foam production. The greenhouse gas reductions for the non-isocyanate microalgae polyurethane pathway are slightly lower at 58% compared with conventional polyurethane foam. However, it offers additional benefits by reducing toxicity potential compared to the isocyanate polyurethane pathway. The analysis also included a biorefinery-level analysis to evaluate the impact of incorporating polyurethane production into fuel-processing microalgae biorefineries. The sensitivity analyses conducted in this study reveal that improved algae cultivation strategies can lead to decreases of up to 127% and 80% in GHG emissions from the baseline process of Bio-PU and Bio-NIPU, respectively. Likewise, implementation of renewable electricity can result in up to 128% and 74% lower GHG emissions compared to the baseline production of Bio-PU and Bio-NIPU, respectively. Finally, the analysis evaluated different coproduct handling methods including displacement and allocation (based on mass, energy, and market-value). The results suggest that it is important to consider both the displacement and allocation methods as these led to significant differences in the environmental impacts.

Received 26th August 2025
Accepted 18th November 2025

DOI: 10.1039/d5su00708a

rsc.li/rscsus

Sustainability spotlight

This study presents a life cycle analysis for two biobased polyurethane (Bio-PU) pathways that may be derived from microalgae, including a novel non-isocyanate (Bio-NIPU) route offering a means of avoiding toxic isocyanate inputs. The analysis offers valuable insights into how the impacts of the proposed technologies compare to conventional polyurethane and highlights the contribution of the various process stages. The findings indicate that Bio-PU and Bio-NIPU reduce GHG emissions by 79% and 58%, respectively, compared to conventional PU. Additionally, fossil energy consumption decreases by 41% and 15%, respectively. However, water consumption is higher compared to conventional PU. Sensitivity analyses reveal that alternative algae cultivation strategies, renewable energy, and modifications in chemical inputs could further reduce the GHG emissions of microalgae-based PU. The analysis would particularly benefit from further research on utilizing alternative chemicals and formulation approaches, especially for Bio-NIPU.

1 Introduction

Polyurethane (PU) is a plastic material with a diverse product portfolio that includes insulation of refrigerators and buildings, cushioning furniture and mattresses, adhesives, car molding, tires, shoe soles, and sportswear. This material is conventionally made from the reaction of an organic isocyanate such as toluene diisocyanate (TDI), methylene diphenyl isocyanate (MDI), and polymeric isocyanates (PMDI) with compounds containing multiple hydroxyl groups or polyols.[1,2] The precursors utilized directly affect the properties of the final PU product and what applications it may be suited for.[3] Natural gas and crude oil are the major sources of carbon for the building blocks used in the production of conventional PUs. In 2023, the PU

[a]*Systems Assessment Center, Energy Systems and Infrastructure Analysis Division, Argonne National Laboratory, 9700 South Cass Avenue, Lemont, IL, 60439, USA. E-mail: pbenavides@anl.gov*

[b]*Catalytic Carbon Transformation and Scale-up Center, National Renewable Energy Laboratory, 15013 Denver West Parkway, Golden, CO, 80401, USA*

production in North America reached a total of 4.1 million tonnes (MMT) that required the approximate consumption of 3.0 MMT of crude oil and natural gas.[4,5] These statistics highlight the importance of diversifying the feedstocks for PU production; incorporating biobased sources, such as algae, could make an important contribution to this effort.

Biobased PU (Bio-PU) has been successfully produced from lignocellulosic materials, vegetable oils, algae, and waste products.[6–8] Several conversion processes convert the biobased feedstocks to polyols, which then react with isocyanates. However, isocyanates are being increasingly regulated due to their associated health hazards.[9,10] Therefore, alternative routes that prevent the use of isocyanates such as the production of non-isocyanate polyurethane (NIPU), have been under development. These NIPU synthesis routes use cyclic carbonates that can be obtained from epoxidized vegetable oils.[11] Other oil sources, like microalgae, are good biobased feedstocks for NIPU production due to their high content of polyunsaturated fatty acids and triglycerides (TAG). NIPUs produced from microalgae oils have demonstrated similar prices to conventional PU, which are further reduced by economies of scale.[12] Additionally, microalgae as a feedstock do not compete with land use with crops, have a high photosynthetic efficiency, and are capable of growing in both freshwater and saline water. More importantly, microalgae can be used to produce fuel and high-value chemicals through biorefinery processes designed for converting biomass.[13]

Life-cycle analysis (LCA) can be used to estimate the energy and environmental benefits and potential tradeoffs of these microalgae biorefinery models and alternative algae-based PU pathways. Early stage LCA studies focused mostly on estimating the environmental impacts of algal biomass growth, which later broadened their scope to microalgae biorefineries focused on producing biofuels and bioenergy.[14–18] Other LCAs looked at the inclusion of other products like proteins, pigments, and bioplastics (*i.e.*, polylactic acid).[14,19–21] Different authors[14,15,19] have pointed out the variety of the methods used in these LCAs and the need for a clear definition of the strategies to estimate the environmental impacts of individual products, considerations of the carbon uptake, and the effect of the recycling streams in microalgae biorefineries. Interestingly, to date there are very few LCA studies[22–25] incorporating PU foam as a coproduct in microalgae biorefineries or that analyze the environmental impacts of microalgae-based PU foams.

Therefore, this paper provides stakeholders with insights into the environmental impacts of microalgae-based PU by presenting a comprehensive comparison of the greenhouse gas (GHG) emissions, fossil energy consumption, and water consumption, *via* LCA, of two pathways: Bio-PU and biobased NIPU (Bio-NIPU). The first pathway consists of the production of polyols from microalgae TAG and subsequent synthesis of flexible PU foam by a process similar to conventional production, while the second pathway considers the transformation of TAG into a rigid PU foam without the addition of isocyanates. The primary goals of this study are (1) to evaluate the potential of microalgae-based PU in reducing environmental impacts in comparison to conventional PU and (2) to identify key drivers and energy and environmental hotspots from microalgae-based PU production to inform efforts to improve its environmental profile. Uncertainty is anticipated in the LCA comparison because microalgae-based PU is at a lower technology readiness level than conventional PU.[26] This study also evaluates the substitution of nutrients and chemicals and the implementation of different coproduct handling methods in the estimation of the environmental impacts of microalgae-based PU foams. In addition, this analysis provides an opportunity to compare the benefits and trade-offs of a biorefinery process co-located with an algae production facility that can focus on the production of renewable fuels and bioproducts.

2 Methodology

2.1 LCA scope

This analysis used the R&D Greenhouse Gases, Regulated Emissions, and Energy Use in Technologies (GREET) model, version 2022,[27] to estimate the cradle-to-gate GHG emissions (kg CO_2e), fossil-energy consumption (MJ), and water consumption (L). For the GHG emissions, the 100-year global warming potential (GWP) values defined in the Intergovernmental Panel on Climate Change (IPCC)'s 6th Assessment Report (AR6) were used: one for CO_2; 29.8 for methane (CH_4); and 273 for N_2O.[28] The R&D GREET model defines the water consumption as the "net water use" calculated by subtracting the amount of water returned to natural reservoirs from the gross water consumption in the system boundary; this definition is consistent with the ReCiPe 2016 [Midpoint, Hierarchist (H)] method.[29] Consistent with previous research,[30] this study considers water consumption to be associated only with fresh water. Details on the incorporation of saline water can be found in previous reports.[20,21] Fossil-energy consumption (FEC) is defined as the net fossil-fuel energy consumed throughout the pathway, which is consistent with the definition used in the cumulative energy demand (CED) method.[31] The study has a geographical scope of the United States, utilizing 2022 state-of-technology data to develop the life cycle inventory.[32] The data were obtained through process simulations and direct experimental measurements and were based on annual average processing rates (seasonal variations were not considered in this study).

Fig. 1 shows simplified process flow diagrams of the microalgae biorefinery pathways analyzed in the study: (A) Bio-PU and (B) Bio-NIPU. These pathways, based on an example high-carbohydrate *Scenedesmus* composition, convert algal biomass into four coproducts (renewable diesel, renewable naphtha, electricity, and PU foam), three recycled products (recycled CO_2 sent to the cultivation stage and recycled nitrogen and phosphorus to offset fresh ammonia and diammonium phosphate [DAP] demands in the cultivation stage), and anaerobic digestate. As observed in Fig. 1, the use and end-of-life stages are excluded from the analysis, as these are assumed to be similar among conventional PU, Bio-PU, and Bio-NIPU.

The results are presented from both product-level and biorefinery-level analyses to better understand the system-wide environmental effects of the biorefinery. The product-level analysis focuses on the environmental impact of a specific

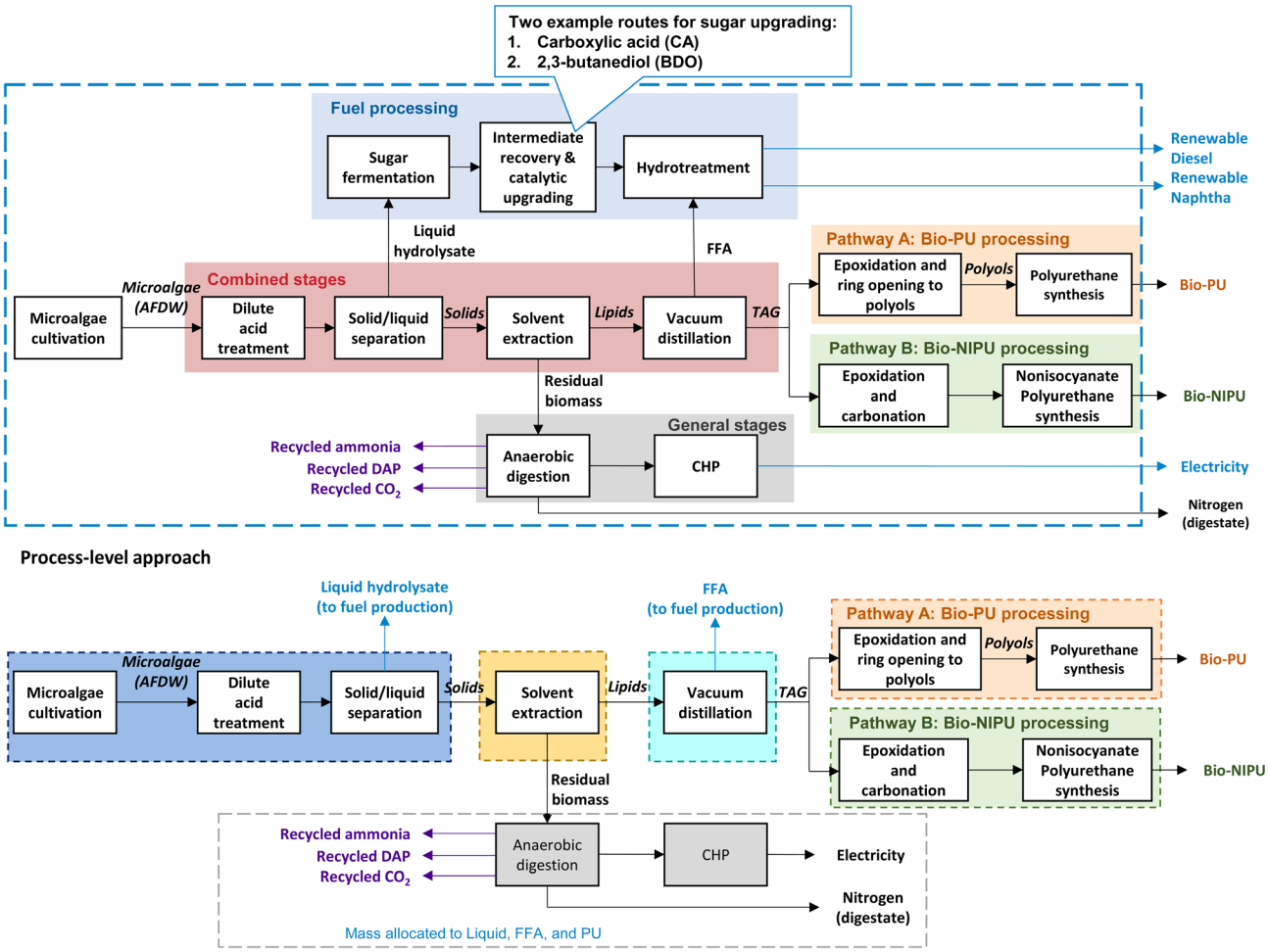

Fig. 1 System boundary of the algae biorefinery for the two pathways analyzed: (A) Bio-PU and (B) Bio-NIPU. Upper diagram: system-level approach; lower diagram: process-level approach. FFA: free fatty acids, CHP: combined heat and power, AFDW: ash-free dry weight, DAP: diammonium phosphate, TAG: triglycerides, Bio-PU: biobased polyurethane, and Bio-NIPU: biobased non-isocyanate polyurethane.

product, while the biorefinery-level analysis examines the environmental impacts of the entire biorefinery system, including both the main product and coproducts. Both system-level and process-level approaches have been employed for the product-level analysis.

2.1.1 Product-level LCA. This analysis focuses on microalgae-based PU foam as the primary product of the biorefinery as opposed to fuel, which has been the focus of previous assessments;[22,33,34] therefore, a functional unit (FU) of one kg of Bio-PU or Bio-NIPU was used depending on the pathway analyzed. Based on the processes and product properties of the two microalgae-based PU pathways,[12,22] their environmental impacts were compared to those of the corresponding conventional PU foam. For the Bio-PU pathway, its impacts were compared with those of flexible PU foam, while the impacts of the NIPU pathway were compared with those of rigid PU foam. This is because in Bio-PU, the reaction between the isocyanate and the polyols produces a more flexible foam, whereas in Bio-NIPU, cross-linking between carbonate groups and hexane diamine leads to the formation of a rigid foam.[12,35] The environmental impacts of the conventional flexible and rigid PU foam were also obtained from R&D GREET.[27]

The biorefinery evaluated here produces both fuel and chemical products. This can pose a challenge when evaluating the emission and energy impacts of either the fuel or the chemical. Therefore, two approaches are proposed to conduct the LCA specific to Bio-PU and Bio-NIPU, the system-level, using displacement, and the process-level, using mass allocation at each stage of the process; which are consistent with previous work by Cai *et al.*[36]

2.1.1.1 System-level approach. The displacement method used in this approach consists of assigning the entire environmental impacts of the biorefinery to the PU foam and subtracting the credits from the avoided impacts of the life cycle of conventional products displaced by the other coproducts of the biorefinery. For instance, renewable diesel and renewable naphtha displace the production and combustion of conventional diesel and gasoline blendstock, respectively, and the electricity from CHP replaces the generation of average U.S. grid electricity. The environmental impacts associated with these displaced products are shown in Table S1 of the SI.

2.1.1.2 Process-level approach. This approach only includes the stages involved in the production of PU foam (dilute acid treatment, solid/liquid separation, solvent extraction, vacuum distillation, and Bio-PU or Bio-NIPU processing) and uses mass allocation to distribute the environmental burdens among the outlet streams of each stage (colored blocks in the "process level approach" section in Fig. 1). Mass allocation was chosen as the coproduct handling method because the analysis focused on a chemical product (Bio-PU or Bio-NIPU). Pretreatment and vacuum distillation were the only stages that required the allocation of environmental impacts between the outlet streams. In contrast, the environmental impacts of the solvent extraction stage were only allocated to the lipid stream to avoid "allocating away" impacts to the residual biomass waste stream. The credits from exported electricity and the use of the digestate as a soil amendment (dotted gray line box in the "process level approach" section in Fig. 1) were allocated by mass to the coproducts (liquid hydrolysate, free fatty acids [FFA], and the PU foam). Life cycle inventory data adapted for this approach are provided in Section S2 of the SI.

2.1.2 Biorefinery-level LCA. The biorefinery-level analysis evaluated the GHG emissions of all biorefinery products (Bio-PU or Bio-NIPU, renewable diesel, and renewable naphtha) and compared them with their corresponding conventional counterparts' production. In this analysis, the FU was determined based on the highest yields of the coproducts from the two sugar upgrading routes. Therefore, the biorefinery-level LCA for Bio-PU employed a FU of the production of 3.6 tonnes of PU, 97 GJ of renewable diesel, 51 GJ of renewable naphtha, and 21 GJ of electricity. Likewise, the FU for the analysis of Bio-NIPU considered the production of 4.5 tonnes of PU, 97 GJ of renewable diesel, 51 GJ of renewable naphtha, and 15 GJ of electricity. Certain routes that did not yield the quantity of coproduct specified by the FU (*i.e.*, yield of renewable diesel in the 2,3-butanediol [BDO] route) compensated for the deficit by incorporating the corresponding conventional counterpart (see Table 1).

The total GHG emissions from the biorefinery were distributed by mass among the three major coproducts (Bio-PU or Bio-NIPU, renewable diesel, and renewable naphtha) excluding electricity, whose effect was later incorporated in the comparison with the conventional counterparts. Mass allocation was used in this perspective because it directly uses the mass yields and reduces uncertainty due to price fluctuation (if market value were used instead). The methodology used to estimate the GHG emissions for renewable diesel and renewable naphtha differed from that for Bio-PU and Bio-NIPU. This disparity is due to variations in the carbon credit accounting between fuels and plastics. For instance, according to ISO 14067,[37] carbon sequestration credits are only included when PU is the coproduct, as the carbon dioxide can be stored in the polymer for a period of time. In contrast, when fuel is the coproduct, no carbon sequestration credits are included because the carbon dioxide, stored in microalgae, will be combusted and released into the atmosphere upon using the fuel. To estimate the total GHG emissions of the conventional counterparts, the GHG emissions of the life cycle of petroleum diesel, gasoline blendstock, electricity, and flexible or rigid PU (Table S1 in the SI) were multiplied by the quantity of coproducts from Table 1 and added up.

2.2 Open pond microalgae cultivation and biorefinery operation overview

2.2.1 Microalgae cultivation and biorefinery description. As depicted in Fig. 1, the process begins with the growth of microalgae biomass, which consists of open pond cultivation and dewatering. The inventory data for cultivation (see Table S2 in the SI) were consistent with the 2022 State of Technology report for algae biomass production from the National Renewable Energy Laboratory and included a microalgae productivity of 18.5 g m^{-2} day^{-1}.[32,38] The model used performance data from cultivation tests using saline water carried out for one year in Arizona, extrapolated to temporal conditions in Florida primarily with respect to net water evaporation rates.[22,32] After cultivation, the conversion biorefinery consists of four major processing sections: (1) dilute acid pretreatment, solid/liquid separation, lipid extraction, and lipid separation ("combined stages" whose operations are necessary for the production of both fuels and PU products), yielding intermediate feedstocks for fuel (liquid hydrolysate and free fatty acids [FFA]) and PU

Table 1 Quantity of biorefinery coproducts and conventional counterparts used for the biorefinery-level LCA comparison[a]

Pathway		Bio-PU			Bio-NIPU		
Route		CA	BDO	Conventional counterparts	CA	BDO	Conventional counterparts
Diesel (GJ)	Renewable	97.3	89.0	—	97.3	89.0	—
	Conventional	—	8.3	97.3	—	8.3	97.3
Naphtha (GJ)	Renewable	40.3	51.4	—	40.3	51.4	—
	Conventional	11.1	—	51.4	11.1	—	51.4
Bio-PU (tonnes)		3.6	3.6	—	—	—	—
Bio-NIPU (tonnes)		—	—	—	4.5	4.5	—
Conventional PU (tonnes)	Flexible	—	—	3.6	—	—	—
	Rigid	—	—	—	—	—	4.5
Grid electricity (GJ)		2.9	—	21.0	2.9	—	15.0

[a] Note. CA: carboxylic acid route and BDO: 2,3-butanediol route.

upgrading (TAG); (2) sugar fermentation and upgrading plus hydrotreating ("fuel-only" processing stages), (3) epoxidation of TAG and synthesis of PU ("Bio-PU" or "Bio-NIPU" processing pathways), and (4) supporting operations enabling the recovery of energy and nutrients through anaerobic digestion (AD) from residual biomass and combined heat and power (CHP) generation ("general stages"). For the fuel-only processing stages, two fermentation routes from the liquid hydrolysate were considered: one producing carboxylic acids (CA) and another generating BDO, with either fermentation intermediate product subsequently processed through a series of catalytic upgrading steps to produce hydrocarbon fuels.[22] The effect of these two options on the environmental impacts of the microalgae-based PU foams was evaluated in this study. The biorefinery was modeled in Aspen Plus to estimate the requirement of materials and energy sources.[12,22,39] Tables S3 and S4 in the SI show the material and energy requirements for a biorefinery processing approximately 384 tonnes of ash-free dry weight (AFDW) microalgae biomass per day under different routes of sugar upgrading and pathways for PU foam polymerization.

2.2.2 Bio-PU and Bio-NIPU production from TAG. For the production of Bio-PU, formic acid, hydrogen peroxide, and other chemicals were combined with TAG to produce polyols *via* epoxidation and ring opening, which were reacted with TDI and other chemicals to produce flexible foam *via* commercially mature technology.[40] In the Bio-NIPU process, TAG was reacted with acetic acid, hydrogen peroxide, and a catalyst and mixed with toluene for epoxidation. After separation of the catalyst and recovery of toluene, the epoxidized TAG was carbonated with carbon dioxide (CO_2) and a tetrabutylammonium bromide catalyst to generate a carbonated oil, which was polymerized with foaming agents (ammonium bicarbonate and citric acid) and hexane diamine to obtain a rigid PU foam.[12] This modeled process for Bio-NIPU is based on an earlier proof-of-concept technology reported by Dong *et al.*,[12] and the authors acknowledge that this technology is in continuous development. Recent research has indicated that certain process modifications, such as the use of alternative diamine monomers and foaming methods, may result in more optimal reaction rates and product properties. At the time this manuscript was submitted, an alternative version of this process had been published using ethylene diamine and an alternative foaming method;[23] however, because this work was conducted in parallel, the original process assumptions reported in Dong *et al.*[12] are maintained. More detailed descriptions of the microalgae cultivation and the biorefinery stages are available in previous literature.[12,22,40,41]

2.2.3 Nutrient recovery and energy generation. The biorefinery also recovered nitrogen and phosphorus, which were used as nutrients for microalgae cultivation, and processed the residual biomass through AD to produce biogas and digestate (EPA Class A biosolid). The process generated energy *via* CHP using the biogas from AD, which was used internally. The electricity generated by the CHP system fulfilled the power requirements of the biorefinery, with a surplus amount exported to the grid, for which displacement credits were accounted. It was assumed that the digestate was exported for a soil amendment and the CO_2 generated in the biorefinery was recycled back to the cultivation stage. The environmental impacts of the chemicals used in the process were estimated either by developing their life cycle inventory data from the literature (see Section S3 in the SI) or by taking them from R&D GREET.

2.2.4 Carbon uptake and digestate utilization. The microalgae cultivation used CO_2 supplied from a point source by pipeline; therefore, the estimation of the GHG emissions of Bio-PU and Bio-NIPU accounted for credits from the carbon stored within the PU foam that otherwise would have been released to the atmosphere. This is because this study assumed that the carbon credit for captured CO_2 is given to the algae biorefinery and not to the CO_2 source.[42] Because the other chemicals (*i.e.*, TDI, hexane diamine, *etc.*) contributing to the process were fossil-carbon sources, a carbon balance was carried out to estimate the carbon uptake within Bio-PU and Bio-NIPU. According to the carbon balance (see SI Section S4) the carbon uptake content was 0.48 and 0.42 kg C per kg of Bio-PU and Bio-NIPU, respectively. It should be noted that even though Bio-NIPU sequesters additional carbon during the carbonation stage, the carbon uptake is higher for Bio-PU, because, under the modeled assumptions, microalgae TAG comprises a larger portion of the final Bio-PU product than Bio-NIPU. The recycling of some of the byproducts (ammonia and DAP from the AD effluent, and CO_2) from the biorefinery to the cultivation stage, helped offset the need for external fertilizer and CO_2 inputs. In the CA route, the recycled byproducts fulfilled 42, 72, and 71% of the CO_2, ammonia, and DAP requirements, respectively; while in the BDO route, these requirements were met by 52, 71, and 52% for CO_2, ammonia, and DAP, respectively.

The application of digestate to soil, due to the nitrogen content in its solids, can substitute the application of other conventional nitrogen sources.[43] This study assumed that the AD digestate is centrifuged and used as a soil amendment by nearby agricultural operations, thereby displacing the use of calcium nitrate,[22] as reported by previous research.[44] The centrifuge uses 0.101 kWh and 5 g of acrylonitrile-butadiene-styrene polymer per dry kg of digestate.[43] Tables S3 and S4 in the SI show that per kg of Bio-PU, 4 g of nitrogen in the digestate can replace up to 31 g of calcium nitrate. Similarly for a kg of Bio-NIPU, the digestate contains 5 g of nitrogen, displacing up to 25 g of calcium nitrate. It was assumed that 20% of the carbon content in the digestate was sequestered in the soil upon application, resulting in 74 g C sequestered per dry kg of digestate.[43] The remaining 80% of the carbon content was primarily released as CO_2; however, as these are biogenic carbon emissions they were not included in the estimations.[45] Additionally, a negligible amount of CH_4 (10 mg CH_4 per dry kg of digestate) is emitted during digestate application, but this was also excluded from the calculations.[27,43]

2.3 Scenario, sensitivity, and uncertainty analyses

2.3.1 Scenario analyses. The scenario analysis provides insights into the effect of modifications to the process conditions and the LCA methodology. Each modification is evaluated

independently to isolate its specific effects. Four scenario analyses were conducted in this study. The first one, algae cultivation strategy, compared the microalgae cultivation state-of-technology (SOT) in 2022 (baseline)[32] with a future scenario for the year 2030 that involves improvements based on reductions of the energy requirements in the open pond cultivation and CO_2 sourcing (2030 target projection).[33] The inventory data of the current and futuristic comparison are provided in Section S5 of the SI. The second scenario analysis assessed the influence of renewable energy on GHG emissions, accomplished through the substitution of electricity from the average US grid with wind power and the replacement of fossil-based natural gas with renewable natural gas (RNG) from wastewater sludge. This analysis did not account for the infrastructure impacts associated with wind power generation, and thus, it is assumed that wind power does not generate GHG emissions. Additionally, in the RNG scenario analysis, the biogenic CO_2 emissions credits (56 g CO_2 per MJ) from RNG combustion were subtracted from the CO_2 emissions associated with the combustion of fossil-based natural gas.[27,46] The third scenario analysis evaluated changes in the chemicals used in the process. One of these analyses considered shifting the nitrogen source from ammonia to urea on a 1 : 1 nitrogen mass basis. In addition to potential GHG reductions, a motivation for this scenario is that using urea may result in higher CO_2 uptake efficiency under optimal pH conditions. Under these conditions, 1.76 kg of urea had a similar nitrogen content to one kg of ammonia. Because urea is also a source of fossil carbon for algae growth, the requirements of sparged CO_2 were reduced to maintain a fixed carbon input in the cultivation. This scenario analysis also considered the substitution of conventional ammonia (baseline) with other types sourced from alternative carbon feedstocks (green ammonia) and captured CO_2 (blue ammonia)[47] and investigated recent improvements in the Bio-NIPU production technologies by replacing the use of hexane diamine with biobased pentane diamine. The production of biobased pentane diamine has been successfully achieved at large scale and reported lower GHG emissions than other fossil-based diamines (*i.e.* hexane diamine and ethylene diamine). Inventory data for the production of Bio-NIPU with biobased pentane diamine are presented in Tables S15 and S16 of the SI.

The fourth scenario analysis evaluated the GHG emissions results based on different coproduct handling methods including system expansion and allocation based on their energy content, market value (revenue), and a hybrid method combining mass allocation with displacement of coproduced electricity. The energy content and market values are based on GREET and other literature studies[22,48–51] and are summarized in Tables S17 and S18. A synthetized depiction of the four coproduct handling methods employed in this study is presented in Table S19 of the SI. All four scenario analyses were applied to the product-level LCA, while only the renewable electricity and changes in chemicals scenario analyses were evaluated for the biorefinery-level LCA.

2.3.2 Sensitivity analysis. The scenario analysis examines variations in GHG emissions for Bio-PU and Bio-NIPU by adjusting one input parameter at a time using a defined variation ratio. Based on other algae-based bioproduct analyses[52] this study assumed a ±50% variation in energy and material inputs associated with the production of Bio-PU and Bio-NIPU. The resulting GHG emissions were compared to those of the product-level LCA baseline, and the percentage of variation was calculated and reported.

2.3.3 Uncertainty analysis. The uncertainty analysis evaluates the effect of variability in process parameters on the GHG emissions of Bio-PU and Bio-NIPU. For instance, the lipid content of microalgae is expected to vary depending on the cultivation conditions or the nature of the species, which affects the requirement of microalgae biomass per kg of microalgae-based PU foam. To account for this uncertainty, a ±50% range of variation in microalgae biomass input relative to the baseline was assumed.[23,52] For Bio-NIPU, the use of different diamines, such as hexane, pentane, or ethylene diamine, can influence the yield. Therefore, the uncertainty analysis also considered a ±50% variation in diamine usage per kg of Bio-NIPU compared to the baseline. To estimate the GHG emission range under uncertainty for microalgae-based PU foams, 5000 Monte Carlo simulations were performed, using a triangular distribution for the microalgae biomass and diamine inputs per kilogram of Bio-PU and Bio-NIPU. The simulation results were analyzed to identify the 10th and 90th percentiles which were defined as the upper and lower bounds of the GHG emission range for microalgae-based PU.

3 Results

3.1 Product-level and biorefinery-level GHG emissions

3.1.1 Product-level LCA. Fig. 2A and B show the GHG emissions from the production of Bio-PU and Bio-NIPU across the different approaches and their comparison with their conventional counterparts. The GHG emissions for Bio-PU and Bio-NIPU are considerably lower compared to those from conventional PU foam. The values of the GHG emissions ranged between 0.72 and 1.43 kg CO_2e per kg for Bio-PU, reflecting a decrease of 58–79% compared to conventional flexible foam. For Bio-NIPU the GHG emissions ranged from 1.35 and 1.90 kg CO_2e per kg, indicating a reduction of 41–58% compared to conventional rigid foam. The highest GHG emission values were obtained in the system-level BDO route, primarily because of its higher requirements for natural gas (see SI Tables S3 and S4) and chemicals, such as corn steep liquor, compared to the CA route. In comparison with conventional PU, Bio-NIPU offers additional advantages apart from GHG emission reduction. Its production does not involve the use of phosgene and isocyanates, which reduces the toxicity and health hazards associated with conventional PU production[53] and ensures compliance with mandates restricting the use of isocyanates in the chemical industry.[54] Although evaluating these impacts is beyond the scope of this analysis, future LCA studies could quantitatively estimate the potential benefits of Bio-NIPU over Bio-PU and conventional PU by analyzing impacts such as human toxicity and ecotoxicity potential. For example, toluene diisocyanate (TDI) has been reported to cause acute respiratory effects in humans when inhaled at concentrations exceeding 80 ppb or

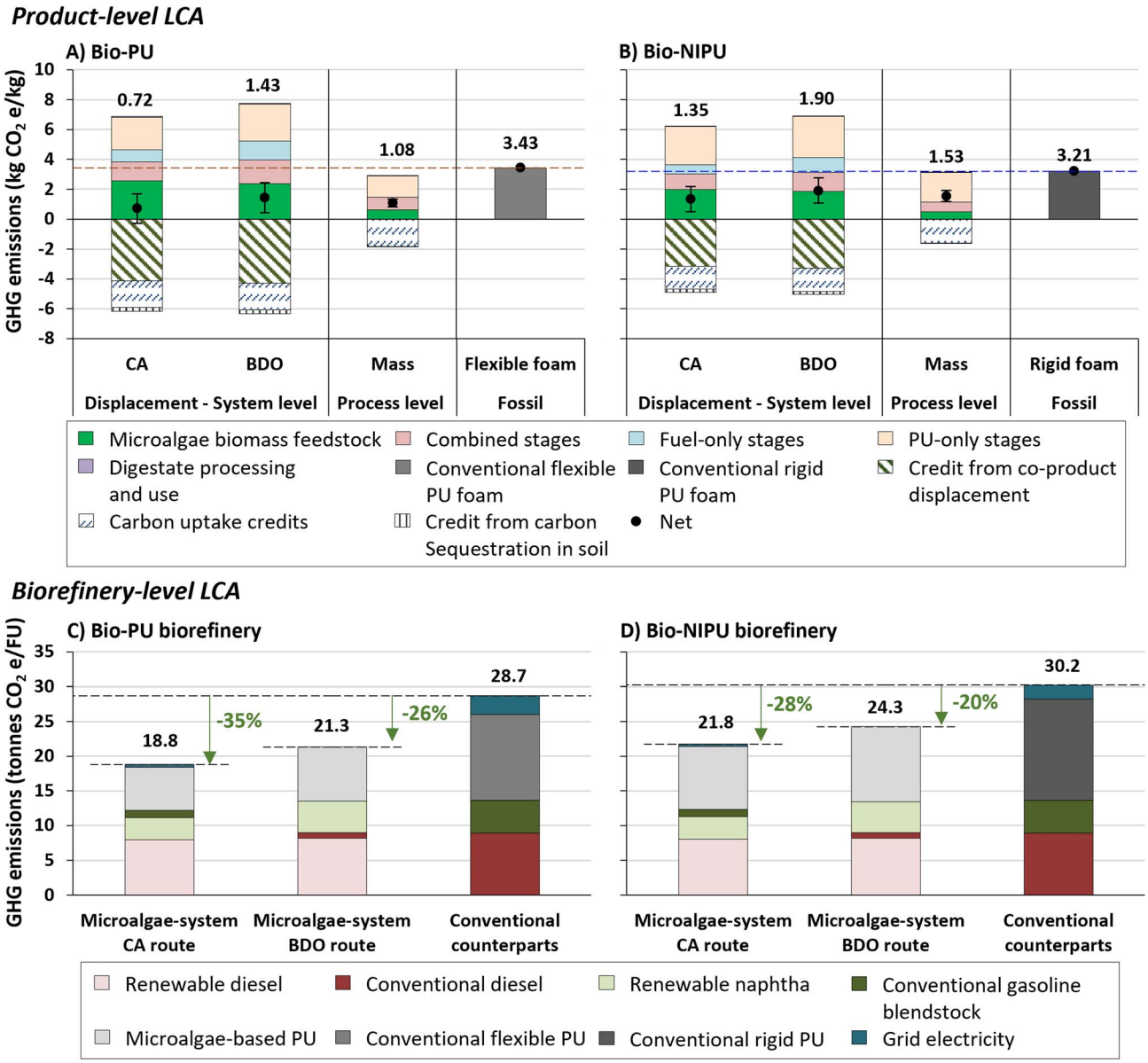

Fig. 2 GHG emissions at the product-level analysis for (A) Bio-PU and (B) Bio-NIPU and at the biorefinery-level analysis for (C) Bio-PU and (D) Bio-NIPU. The orange and blue dashed lines in the product-oriented LCA indicate the GHG emissions of conventional flexible and rigid PU foam, respectively. The credit from coproduct displacement comprises the avoided emissions for the production and combustion of conventional diesel and gasoline blendstock and generation of grid electricity. The digestate processing and use includes the GHG emissions associated with centrifugation of the digestate. The credits from carbon sequestration in soil are due to the use of the digestate from AD as soil amendment. CA: carboxylic acid, BDO: 1,3-butanediol, and PU: polyurethane.

during prolonged exposure to lower doses (20 ppb).[55] Additionally, the Integrated Risk Information System (IRIS) has documented chronic lung-function decline at inhalation exposure concentrations above 7×10^{-5} mg m^{-3}.[56] In contrast, no such exposure-related health risks have been reported for hexane diamine, indicating that these risks could be avoided when using Bio-NIPU as an alternative.[57]

An analysis of the material and energy feedstocks (see Fig. S2 in the SI) shows that microalgae biomass and natural gas are the major contributors to GHG emissions in the process. Depending on the case evaluated, the microalgae biomass contributes up to 37 and 32% of the GHG emissions of Bio-PU and Bio-NIPU (displacement–CA route for both), respectively, while natural gas contributes to up to 38 and 34% of the GHG emissions of Bio-PU and Bio-NIPU (displacement–BDO route for both), respectively. Besides, some chemicals showed important contributions to the GHG emissions. For instance, in Bio-PU production, TDI contributed up to 25% of the GHG emissions (process-level), while in the case of Bio-NIPU, hexane diamine contributed up to 36% of the GHG emissions (process-level). Another important component of the GHG emission results is the credits from carbon uptake which are estimated at 1.78 and 1.55 kg CO_2e per kg of Bio-PU and Bio-NIPU, respectively.

These credits were included in the GHG emission accounting based on the assumption that Bio-PU and Bio-NIPU have high chemical stability and would degrade very slowly under typical landfill storage conditions after disposal. However, it is important to note that formal laboratory tests have not yet been conducted to confirm this behavior. Biodegradation of biobased polyurethane thermosets would require specific conditions such as those found in composting, or during enzymatic, thermal, and microbial degradation. The evaluation of these conditions is beyond the scope of this study.[58–61]

The GHG emissions associated with PU production are lower for Bio-PU compared to Bio-NIPU. However, the total material and energy requirements (process-related GHG emissions) per kg of PU foam (solid stacked bars in Fig. 2A and B) are higher for Bio-PU than for Bio-NIPU. This discrepancy arises from the lower yield of Bio-PU in biorefineries, which is approximately 21% less than that of Bio-NIPU; however, the lower yield for Bio-PU also results in higher coproduct GHG emission credits per unit of PU product output compared to Bio-NIPU. Furthermore, the process-related GHG emissions for Bio-PU are lower than those for Bio-NIPU, because the chemicals used in the Bio-PU pathway contribute to reduced emissions compared to those utilized in the Bio-NIPU pathway (see Section S6.1 in the SI). This, combined with the higher coproduct GHG emission credits ultimately leads to overall lower GHG emissions for Bio-PU in comparison to Bio-NIPU. Substituting certain chemicals, such as fossil-based hexane diamine with alternative biobased diamines, could reduce the process-related GHG emissions for Bio-NIPU production, thereby compensating for the reduced GHG emissions coproduct credits; this is further explored in Section 3.3.3.

Fig. 2A and B indicate that the GHG emissions associated with the material and energy requirements of the process-level approach are lower compared to the displacement system-level method applied to the two routes (CA and BDO). This reduction is attributed to the use of mass allocation factors in the analysis of the pretreatment and vacuum distillation stages, which allocate only about half of the impacts from these stages to the PU product. Additionally, the process-level approach excludes the GHG emissions from fuel-only stages. Interestingly, the comparison of three cases in Fig. 2A and B—specifically, system-level displacement applied to the (1) CA route and (2) BDO route, and (3) the process-level approach—reveals that the system-level displacement applied to the CA route achieves lower GHG emissions than the other two cases. This is due to the inclusion of credits from coproduct displacement, whose magnitudes are up to 60% and 50% of the GHG emissions associated with the material and energy requirements for Bio-PU and Bio-NIPU, respectively. This results in comparable GHG emission values across the three cases. It is noteworthy that the overall comparison between system- and process-level approaches may vary depending on the coproduct treatment method employed in the former, as indicated by the scenario analysis results presented in Section 3.3.

Bio-PU and Bio-NIPU generated in a biorefinery utilizing the BDO route for fuel production exhibit higher GHG emissions compared to those produced *via* the CA route, due to the higher natural gas requirements of the BDO route. The fermentation and catalytic conversion steps used to generate and upgrade BDO involve batch fermentation, yielding lower BDO titers, requiring energy-intensive catalytic upgrading of the dilute aqueous stream through the initial dehydration step.[35] In contrast, the CA route employs continuous fermentation with *in situ* acid removal, achieving higher concentrations of the acid product ultimately sent through downstream catalysis steps (although at the expense of complex pertractive membrane separations and solvent recovery steps).[35] Consequently, the BDO route is more energy-intensive than the CA route. These increased process-related GHG emissions from heating are not fully offset by the increased power generation during CHP operations and coproduct GHG emission credits observed in the BDO route. Consequently, the BDO route ultimately resulted in higher net GHG emissions compared to the CA route.

An alternative analysis, presented in Section S6.2 of the SI, evaluates the GHG emissions using a functional unit of one MJ of renewable fuels while viewing PU/NIPU as the coproduct across three different coproduct handling methods (system-level hybrid allocation, system-level market-value allocation, and displacement). The results show a similar trend to those obtained from the PU analysis, with slightly higher GHG emissions observed for the Bio-NIPU pathway compared to the Bio-PU pathway, except when using market price allocation which incurs lower fuel GHG emissions for Bio-NIPU *versus* Bio-PU coproduction, given the higher GHG allocations to the more valuable chemical coproduct. Microalgae-based fuels exhibit lower GHG emissions than fossil fuels (91.4 gCO_2e/MJ), demonstrating reductions of up to 78% for the Bio-PU pathway and 75% for the Bio-NIPU pathway, when the displacement method is applied in the CA route.

3.1.2 Biorefinery-level LCA. The biorefinery-level analysis results for the two pathways and the two sugar upgrading routes are presented in Fig. 2C and D. For the Bio-PU pathway the total GHG emissions associated with the defined FU (3.6 tonnes of Bio-PU, 97 GJ of renewable diesel, 51 GJ of renewable naphtha and 21 GJ of electricity internally-generated and exported to the grid) are estimated at 18.8 and 21.3 tonnes CO_2e for the CA and BDO routes, respectively. The life cycle GHG emissions of similar quantities of the conventional counterparts (PU foam, petroleum diesel and gasoline blendstock) and grid electricity add up to 28.7 tonnes CO_2e. In the Bio-NIPU pathway, the total emissions for the FU (4.5 tonnes of Bio-NIPU, 97 GJ of renewable diesel, 51 GJ of renewable naphtha and 15 GJ of electricity internally-generated and exported to the grid) are estimated at 21.8 and 24.3 tonnes CO_2e for the CA and BDO routes, respectively. Using the same FU, for the conventional counterparts the total GHG emissions are estimated at 30.2 tonnes CO_2e. The comparison with fossil-based counterparts indicates GHG emission reductions of 26 (BDO route) and 35% (CA route), and 20 (BDO route) and 28% (CA route) for Bio-PU and Bio-NIPU, respectively. A look at the coproduct breakdown in Fig. 2C and D indicates that the reductions are mainly due to the difference in the GHG emissions between microalgae-based and conventional PU rather than the differences observed for the

fuels. The carbon uptake credits in Bio-PU and Bio-NIPU led to lower GHG emissions compared to conventional PU foam (see Fig. 2A and B), which resulted in important reductions for the microalgae systems in the biorefinery-level analysis. This suggests that incorporating the production of bioplastics into the microalgae biorefinery reduces its overall environmental impacts.

The biorefinery-level LCA comparison of the two microalgae-based PU pathways indicates that a biorefinery producing Bio-PU achieves greater GHG emission reductions compared to conventional PU than a biorefinery producing Bio-NIPU does, despite lower yields from microalgae for Bio-PU. This suggests that the greater reduction in GHG emissions achieved by Bio-PU relative to conventional PU outweighs its lower yield relative to Bio-NIPU. Therefore, the specific GHG emissions reduction percentage of the microalgae-based PU foam with respect to its conventional counterpart is a crucial factor in assessing the environmental sustainability of these biorefineries.

3.2 Product-level and biorefinery-level fossil energy and water consumption

The results for fossil energy are shown in Fig. S3 of the SI and indicate that the system level displacement–BDO route and the process-level approach have the highest and lowest values, respectively, among all the methods analyzed. The fossil energy consumption of Bio-PU shows a reduction of up to 41% compared to conventional flexible PU, while production of Bio-NIPU can achieve a reduction of up to 15% (process-level for both). Nevertheless, the system level BDO route for Bio-NIPU production shows fossil energy consumption that is 7% higher compared to conventional rigid PU. For both pathways the highest contributor to the fossil energy was the PU only stages; therefore, improvements in those stages, like shifting from fossil to renewable natural gas could potentially reduce both the GHG emissions and fossil energy use of microalgae-based PU foam.

Although the Bio-NIPU pathway has lower fossil energy consumption for natural gas, hydrogen, and ammonia, it results in higher process-related fossil energy consumption than Bio-PU. This is primarily due to the increased use of chemicals specific to the Bio-NIPU production stage, such as hexane diamine, which can account for up to 35% of the total process-related fossil energy consumption. Additionally, Bio-NIPU has lower coproduct credits for fossil energy consumption than Bio-PU. These two factors contribute to the net higher fossil energy consumption of Bio-NIPU compared to Bio-PU, which in some approaches (displacement–BDO route) exceeds that of conventional rigid foam. To mitigate this, employing biobased alternatives for key chemicals in the PU production process could help reduce the fossil energy consumption of the Bio-NIPU pathway.

Fig. S4 in the SI shows the water consumption of the two pathways under analysis. As observed, water consumption, even after the water is recycled, is higher for the two microalgae-based PU pathways in comparison with conventional PU foams. The water consumption in Bio-PU is up to ten times higher compared to conventional flexible PU foam, while that of Bio-NIPU is up to nine times higher compared to conventional rigid PU foam. For both pathways, the fuel-only stages and the combined stages were those with the highest water consumption for the CA and the BDO routes, respectively. Interestingly, the microalgae biomass feedstock did not show the highest water consumption among all the stages. This is because saline water is used for cultivation and the water consumption only accounts for the use of fresh water.

The biorefineries use 18.3 and 29.0 L of make-up process water per kg of Bio-PU and Bio-NIPU, respectively. These values are higher than the total water consumption for conventional flexible and rigid PU foams (5.0 L kg^{-1}). Additionally, certain materials, such as corn steep liquor, have high water consumption, which further increases the overall water consumption of Bio-PU and Bio-NIPU. This is particularly impactful in the CA route, where corn steep liquor contributes to half of the water consumption in the biorefineries due to its increased use in the sugar conversion process. The effects of process water and corn steep liquor explain the higher water consumption observed in microalgae-based PU foams compared to conventional PU foams. However, in cases where this is tied to operational choices such as the type of fermentation nutrient employed, opportunities exist to further improve these results (*e.g.* through the use of alternative nutrient media components such as ammonia in place of corn steep liquor).

3.3 Product-level and biorefinery-level GHG emissions under different scenario analyses

The results of the scenario analyses are presented in Fig. 3 and 4 for the product-level and biorefinery-level LCA, respectively.

3.3.1 Algae cultivation strategy. The comparison between the 2022 SOT assumptions and the cultivation and CO_2 sourcing improvements targeted for 2030 is shown in Fig. 3A and B. As observed, the GHG emissions are reduced by up to 127% for Bio-PU and up to 52% for Bio-NIPU (both reductions in the displacement–CA route) compared to the current SOT basis. The GHG emissions reductions of the 2030 target projection compared to conventional PU foams (dashed lines in Fig. 3A and B) ranged between 75 (process-level) and 106% (displacement–CA route) for Bio-PU and between 58 (process-level) to 80% (displacement–CA route) for Bio-NIPU. Therefore, reaching the targeted projections for year 2030 will result in both higher cultivation productivity and lower GHG emissions for the technology compared to the 2022 SOT.

3.3.2 Renewable energy. The GHG emissions of Bio-PU using renewable electricity ranged from −0.20 to 0.69 kg CO_2e per kg, representing reductions of up to 128% for the system-level approach (CA route) and 36% for the process-level approach baseline (Fig. 3C). The GHG emissions for Bio-NIPU were estimated between 0.35 to 1.11 kg CO_2e per kg, indicating reductions compared to the baseline of up to 74% for the system-level approach (CA route) and 28% for the process-level approach, respectively (Fig. 3D). Most of these reductions were attributed to the lower GHG emissions observed in the algae cultivation stage (see Fig. S5 in the SI). The comparison of the

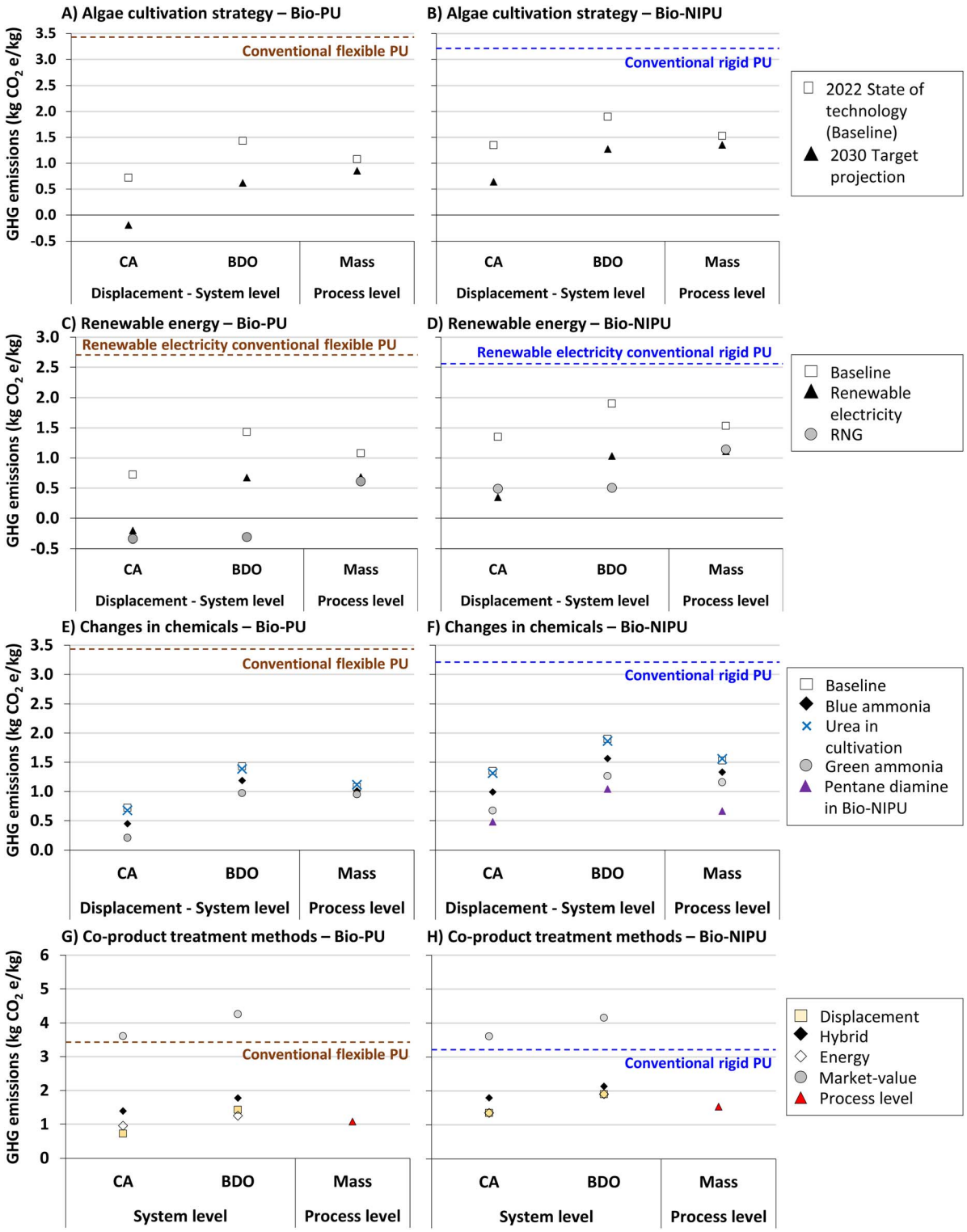

Fig. 3 GHG emissions from the scenario analyses of the product-level analysis: algae cultivation strategy for (A) Bio-PU and (B) Bio-NIPU, renewable energy for (C) Bio-PU and (D) Bio-NIPU, changes in chemicals for (E) Bio-PU and (F) Bio-NIPU, and co-product treatment methods for (G) Bio-PU and (H) Bio-NIPU. The markers indicate the GHG emissions obtained when conducting one sensitivity analysis at a time. The dashed lines indicate the GHG emissions of conventional PU foam. CA: sugar upgrading in fuel production *via* carboxylic acid and BDO: sugar upgrading in fuel production *via* 2,3-butanediol.

GHG emissions between renewable electricity-based Bio-PU and renewable electricity conventional-based flexible PU, showed a reduction of 75–108% in the former, whereas the GHG emissions of renewable electricity-based Bio-NIPU were 57–86% lower compared to renewable electricity-based conventional rigid PU. These findings suggest that as the grid reduces its

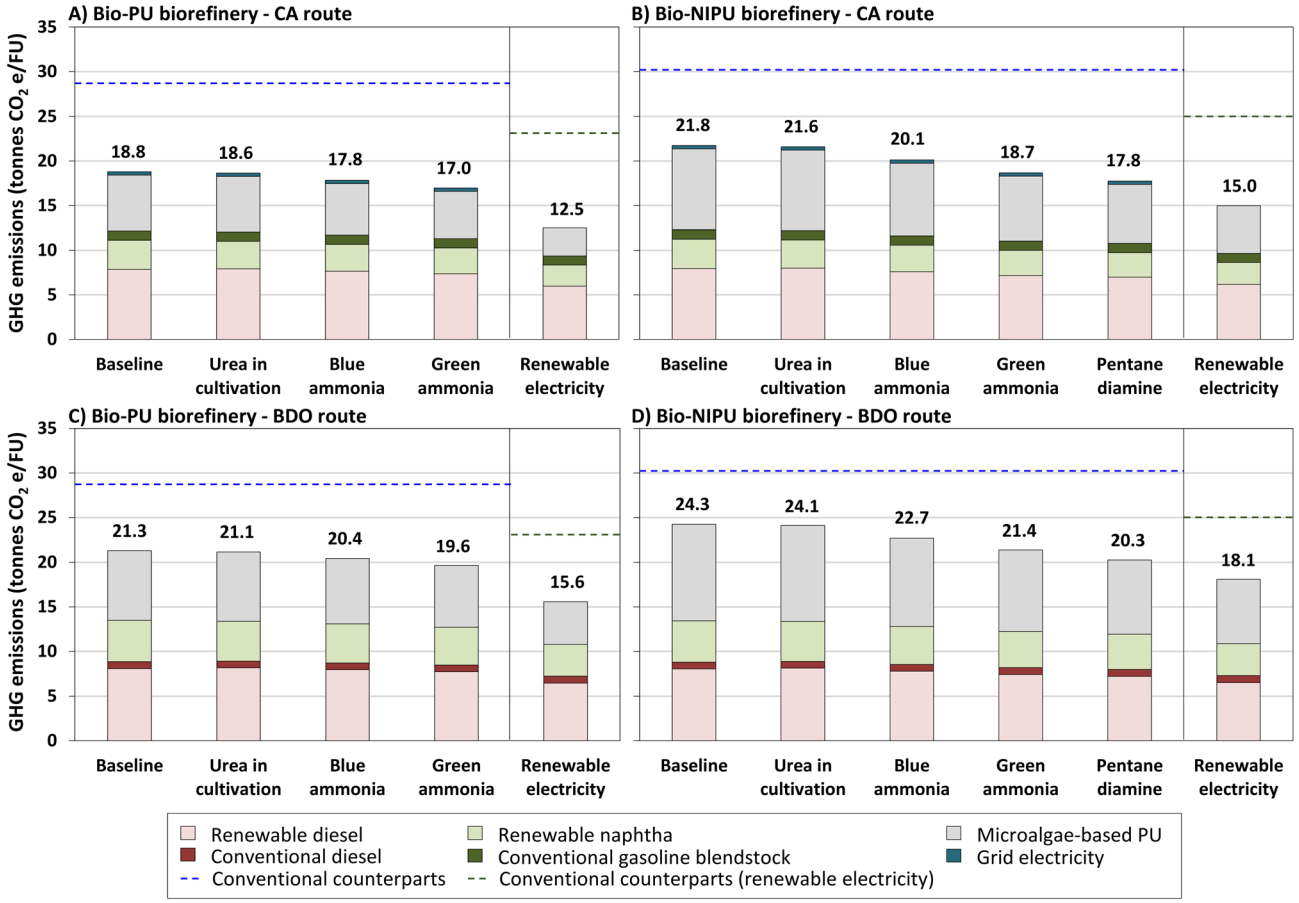

Fig. 4 GHG emissions for the scenario analyses of the biorefinery-level analysis for the CA route: (A) Bio-PU and (B) Bio-NIPU, and the BDO route: (C) Bio-PU and (D) Bio-NIPU. The values indicate the GHG emissions obtained when conducting one sensitivity analysis at a time. The dashed lines indicate the GHG emissions of conventional counterparts.

emissions, microalgae-based PU will become increasingly favorable from a GHG emissions perspective, compared with conventional PU.

The substitution of natural gas with RNG derived from wastewater sludge resulted in lower GHG emissions compared to the baseline. This is because, during RNG combustion, the majority of the CO_2 emitted is biogenic and therefore excluded from GHG emission estimations. Additionally, a credit for avoided emissions from the conventional EOL management of wastewater sludge is subtracted from the emissions associated with the processing of RNG.[46] Under this scenario, the GHG emissions for Bio-PU ranged from −0.34 to 0.61 kg CO_2e per kg, while the GHG emissions for Bio-NIPU ranged from 0.49 to 1.14 kg CO_2e per kg.

Fig. 4A and C indicate that integrating renewable electricity into a Bio-PU biorefinery lowers the GHG emissions associated with producing the FU (3.6 tonnes of Bio-PU, 97 GJ of renewable diesel, 51 GJ of renewable naphtha and 21 GJ of electricity internally-generated and exported to the grid). Specifically, compared to conventional production using renewable electricity, the GHG emissions are reduced by 33 (BDO route) and 46% (CA route) for the FU. For the Bio-NIPU biorefinery (Fig. 4B and D) producing the FU (4.5 tonnes of Bio-NIPU, 97 GJ of renewable diesel, 51 GJ of renewable naphtha and 15 GJ of electricity internally-generated and exported to the grid) with renewable electricity reduces the GHG emissions by 28 (BDO route) and 40% (CA route) compared to renewable electricity-based conventional production of the FU. Similar to the product-level LCA, the biorefinery-level GHG emissions were significantly reduced with the use of RNG (see Fig. S7 in the SI). Furthermore, when RNG was utilized, the GHG emissions of the FU decreased by 48% (both CA and BDO routes) for Bio-PU, and by 41% (both CA and BDO routes) for Bio-NIPU, compared to their conventional counterparts.

3.3.3 Changes in chemicals. The results from shifting the nitrogen source from ammonia to urea are presented in Fig. 3E and F. The variations in GHG emissions between the baseline (ammonia) and the use of urea are only up to 6% for Bio-PU and 3% for Bio-NIPU, across the different methods evaluated. Except for the process-level approach, all the methods show a slight decrease in GHG emissions. These slight variations are due to the tradeoff between the lower emissions of one kg urea compared to ammonia (1.3 and 2.8 kg CO_2e per kg, respectively) and the increased demand for urea to replace ammonia. Due to the small variations observed, shifting the nitrogen source does

not significantly change the comparison of the GHG emissions between microalgae-based and conventional PU foams.

The shift in the Bio-NIPU formulation from hexane diamine to biobased pentane diamine was also examined and the results are presented in Fig. 3F (purple triangle). The GHG emissions of Bio-NIPU with biobased pentane diamine ranged between 0.48 (displacement–CA route) and 1.05 kg CO_2e per kg (displacement–BDO route), which represents GHG emissions reductions of up to 38% (process-level) compared to Bio-PU and of up to 85% (displacement–CA route) compared to conventional rigid PU. This was influenced by the lower requirement (0.187 kg kg^{-1} Bio-NIPU, see Tables S15 and S16 in the SI) and GHG emissions (1.36 kg CO_2e per kg) of the biobased pentane diamine[62] compared to hexane diamine (requirement of 0.206 kg kg^{-1} Bio-NIPU and GHG emissions of 5.47 kg CO_2e per kg). The research on biobased diamines is expanding,[63] and other diamines with low requirements, like ethylene diamine (requirement of 0.13 kg kg^{-1} Bio-NIPU), could also be employed for Bio-NIPU production. This could broaden the opportunities for new Bio-NIPU formulations with significantly improved environmental performance compared to previous and recent synthesis routes using fossil-derived diamines.

Fig. 3E and F also show the results for the comparison of the different ammonia types. While green ammonia is produced from water, air, and renewable electricity, blue ammonia is manufactured from captured CO_2 from industrial processes.[47] The reduction of GHG emissions from conventional to blue ammonia ranged from 6 (process-level approach) to 38% (displacement–CA route) for bio-PU and from 13 (process-level approach) to 27% (displacement–CA route) for Bio-NIPU. However, higher emissions reductions are achieved when green ammonia is used instead of conventional ammonia, ranging from 12 (process-level approach) to 71% (displacement–CA route) and from 24 (process-level approach) to 50% (displacement–CA route) for Bio-PU and Bio-NIPU, respectively due to lower energy requirements and negative process emissions[47] associated with producing green ammonia. In addition, the use of green ammonia reduces the GHG emissions by 72 (displacement–BDO route) to 94% (displacement-–CA route) for Bio-PU and by 61 (displacement–BDO route) to 79% (displacement–CA route) for Bio-NIPU in comparison with their conventional counterparts. Although these results only indicate GHG emission reductions from evaluating one chemical change strategy at a time, simultaneous substitution of two chemicals can lead to further reductions. For instance, producing Bio-NIPU with green ammonia and biobased pentane diamine can result in GHG emissions ranging from 0.02 (displacement–CA route) to 0.63 (displacement–BDO route) kg CO_2e per kg Bio-NIPU. These GHG emissions represent a reduction of between 66 (process-level approach) and 98% (displacement–CA route) compared to baseline Bio-NIPU production.

In the biorefinery-level LCA, both the Bio-PU and Bio-NIPU biorefineries showed larger GHG emission reductions when conventional ammonia was replaced with blue and green ammonia, compared to employing urea in the cultivation stage. The use of green ammonia provided the greatest reductions in GHG emissions among all the chemical sensitivity cases for the Bio-PU biorefinery. These GHG emissions reductions were estimated at 32 (BDO route) and 41% (CA route) compared to conventional production of the FU (Fig. 4A and C). For the Bio-NIPU biorefinery the lowest GHG emission reductions were observed when hexane diamine was substituted with biobased pentane diamine. Under this scenario, the GHG emissions of the FU were 33 (BDO route) and 41% (CA route) lower compared to the conventional production of the FU. These findings highlight the importance that feedstock substitution improvements pose in reducing the emissions of microalgae-based PU.

3.3.4 Coproduct handling methods. Fig. 3G and H show the effect of different coproduct handling methods on the GHG emissions of Bio-PU and Bio-NIPU, respectively. In the system-level approach, the GHG emissions estimated with the market-value allocation have the highest value among the methods used regardless of the pathway used to upgrade the sugars for fuel production. This is because the price of the microalgae-based PU was considerably higher compared to the other coproducts; therefore most of the burdens are allocated to Bio-PU or Bio-NIPU in this case. In contrast, the lowest GHG emissions are observed in the energy allocation *via* CA for both Bio-PU and Bio-NIPU. The reason for this result is that the differences between the energy content of the PU foam are not prominent compared to the other products. These findings indicate a wide variation in results from the different coproduct handling methods employed.

3.4 Sensitivity and uncertainty analyses of GHG emissions in microalgae-based PU foams

3.4.1 Sensitivity analysis. The sensitivity analysis results revealed a direct relationship between the variables. Hence, an increase in a material or energy input led to a corresponding increase in GHG emissions, and *vice versa*. The sensitivity analysis for Bio-PU is presented in Fig. S8A, C, and E of the SI. The results indicate that algae biomass, natural gas, and toluene diisocyanate are the material and energy inputs with the most significant impact on GHG emissions. A variation of ±50% in these inputs results in changes in GHG emissions of up to 263%, 125%, and 50%, respectively, compared to the baseline. The substantial influence of these three inputs is consistent with Fig. S2 in the SI, which shows that they are the major contributors to the GHG emissions of the production process. The findings also indicate that the system-level CA route is more sensitive to these changes compared to the system-level BDO route and the process-level approach. This is a direct result of the combined contributions of GHG emissions per input and the magnitude of the overall GHG emissions of Bio-PU. Other materials, such as ammonia, surfactant, formic acid, and hydrogen peroxide, resulted in Bio-PU GHG emission variations of up to 25%, 18%, 14%, and 11%, respectively. For Bio-NIPU, the sensitivity analysis results are presented in Fig. S9A, C, and E of the SI. Similar to Bio-PU, algae biomass and natural gas are the major inputs influencing the GHG emissions of Bio-NIPU, with variations of up to 111% and 62%, respectively. Additionally, hexane diamine is another significant input, with a ±50% variation leading to up to a 42% change in

the GHG emissions of Bio-NIPU. Interestingly, algae biomass has a greater impact on GHG emission variation in the system-level CA route, while natural gas has a more pronounced effect in the system-level BDO route. These findings highlight potential opportunities for reducing GHG emissions in microalgae-based PU foams. For instance, increasing the lipid concentration in microalgae could reduce algae biomass requirements, while implementing energy-saving practices, such as enhancing heat integration, could lower natural gas consumption. Tabulated data from the sensitivity analysis are available in the SI in Tables S26 and S27, corresponding to Bio-PU and Bio-NIPU, respectively.

3.4.2 Uncertainty analysis. The histograms generated from the Monte Carlo simulations are presented in Fig. S8B, D, and F for Bio-PU, and in Fig. S9B, D, and F for Bio-NIPU. The 90th percentile GHG emissions for Bio-PU are estimated at 1.70, 2.45, and 1.32 kg CO_2e per kg, while for Bio-NIPU, they are estimated at 2.18, 2.76, and 1.90 kg CO_2e per kg, for the system level CA route, system level BDO route and process level approach, respectively. Notably, the highest 90th percentile GHG emissions for both Bio-PU and Bio-NIPU are lower than the GHG emissions of conventional rigid and flexible PU foams used for comparison (3.43 and 3.21 kg CO_2e per kg, respectively). This indicates that the proposed production pathways, even when accounting for some uncertainties in process parameters, can achieve lower GHG emissions compared to the conventional counterparts. The range between the 90th and 10th percentile is indicated in all the cases using error bars in Fig. 2A and B. The corresponding numerical values are presented in Table S28 of the SI.

4 Discussion

This study analyzed the environmental impacts of producing Bio-PU foam along with renewable fuels in a biorefinery processing microalgae biomass. Two different production pathways were evaluated to convert TAG to Bio-PU foam: one generating flexible foam similar to the current industrial practice (Bio-PU), and another synthesizing rigid foam without requiring isocyanates (Bio-NIPU). The GHG emissions of microalgae-based PU foams were lower compared to their conventional counterparts. This outcome was very similar to that observed for fossil energy; however, the water consumption of all microalgae-based PU foams was considerably higher than that of the conventional PU foams. A greater portion of the water consumption was accounted for in the biorefinery processes instead of the microalgae cultivation stage.

The PU synthesis was the stage with higher GHG emissions in both pathways, followed by microalgae cultivation. This study also showed that the transition to more energy efficient cultivation and the substitution of conventional ammonia with green ammonia are strategies that could most beneficially improve the emission profile of bio-PU. Current formulations of Bio-NIPU using biobased pentane diamine also reduced the GHG emissions compared to earlier synthesis pathways using hexane diamine. It was also demonstrated that the choice of coproduct handling method has an important impact on the results. Finally, a biorefinery-level approach proved that incorporating PU foam synthesis into a biorefinery focused on fuel production helped to reduce the overall GHG emissions of the biorefinery products in comparison with producing them through conventional pathways. The analysis performed in this study provided a useful methodology to evaluate the environmental impacts of biochemicals coproduced in biorefineries, highlighted the importance of the methodology chosen for the analysis, and gave important insights to further develop microalgae biorefineries as a strategy to diversify feedstocks for the chemical and fuel industries.

The GHG emissions reported in this study are lower than those previously documented for Bio-PU and Bio-NIPU. For instance, Manzardo *et al.*[64] found that GHG emissions for Bio-PU derived from vegetable oils range from 4.6 to 3.3 kg CO_2e per kg PU which are at least 74% higher than the highest GHG emissions value reported in this study (1.9 kg CO_2e per kg Bio-NIPU). Similarly, the production of bio-based PU from residues such as lignin derived from black liquor or crude glycerol from the transesterification of vegetable oils also resulted in higher GHG emissions than those reported for microalgae-based PU in this study.[65,66] Specifically, the reported GHG emissions for lignin-based PU range from 4.1 to 5.0 kg CO_2e per kg PU,[65] while for crude-glycerol based PU, they range from 4.7 to 7.0 kg CO_2e per kg PU.[66] The higher GHG emissions in these pathways are largely driven by the use of fossil-based methyl diisocyanate in the case of crude glycerol, as well as the low contribution of biobased feedstocks, relative to other inputs, in the lignin-based PU. Liang *et al.*[10] reported that non-isocyanate polythiourethane (NIPTU) derived from biobased 1,4-butanediol is estimated to generate GHG emissions of 3.0 kg CO_2e per kg NIPTU, approximately 57% higher than the highest GHG emissions value reported in this study for Bio-NIPU. It is important to note that the lower GHG emissions of microalgae-based PU, compared to other biobased PUs, may be largely attributed to the biorefinery approach, which allows PU to benefit from credits for fuels and electricity coproduced in the specific biorefinery configurations considered in this study. In contrast, previous studies have reported a standalone PU production facility without such a biorefinery integration approach. Nevertheless, as discussed in this study, the inclusion of PU reduces the environmental impacts not only of the biorefinery but also of the PU product itself.

5 Conclusions

The findings of this study show that microalgae-based Bio-NIPU is a promising route for reducing the toxicity potential of PU production while also reducing GHG emissions. This technology is still under development, offering potential for further reduction of GHG emissions. Additionally, since it relies on electricity as primary energy input, its GHG emissions profile will further improve as the grid lowers its emissions. From microalgae biorefineries, the production of Bio-PU and fuels achieves GHG emission reductions ranging from 26 to 35% compared to conventional production routes. Similarly, the coproduction of Bio-NIPU and fuels reduces GHG emissions by

20–28% compared to conventional production. The GHG emissions of microalgae-based PU are further reduced through the substitution of chemicals. For instance, substituting conventional ammonia with green ammonia can reduce GHG emissions of microalgae-based PU by up to 94% compared to conventional flexible PU, while replacing hexane diamine with biobased pentane diamine can lower the GHG emissions of microalgae-based NIPU by up to 85% compared to conventional rigid PU. By using renewable electricity, the GHG emissions from microalgae-based PU and NIPU are further reduced by up to 108 and 86%, respectively, compared to conventional PU foam produced with renewable electricity. Future research could explore improvements in the lipid to PU conversion process, by reducing the requirements of thermal energy through heat integration and process intensification. Additionally, exploring alternative materials with lower emissions while maintaining comparable yields could be beneficial. To gain a deeper understanding of the implications of Bio-NIPU beyond the impacts evaluated in this study, it is recommended to assess indicators such as human health and toxicity. This could help identify additional benefits of this production pathway.

Author contributions

Ulises R. Gracida-Alvarez: methodology, formal analysis, validation, investigation, visualization, writing – original draft. Matthew Wiatrowski: methodology, investigation, formal analysis, validation, writing – review and editing. Pahola Thathiana Benavides: methodology, validation, supervision, writing – review and editing. Jingyi Zhang: validation, investigation, writing – review and editing. Ryan Davis: conception, validation, writing – review and editing. Troy R. Hawkins: conception, funding acquisition, supervision, writing – review and editing.

Conflicts of interest

There are no conflicts of interest to declare.

Data availability

The life-cycle analysis conducted in this study was performed using the Research and Development Greenhouse gases, Regulated Emissions, and Energy use in Technologies Model (R&D GREET)® available at https://doi.org/10.11578/GREET-Excel-2022/dc.20220908.1.

Additional data supporting this article is included as part of the supplementary information (SI). Supplementary information: detailed life cycle inventories for the Bio-PU and Bio-NIPU biorefineries and chemicals not available in R&D GREET, carbon balance in the biorefinery, life cycle inventories used in the scenario analysis, and additional figures and tables. See DOI: https://doi.org/10.1039/d5su00708a.

Acknowledgements

The authors acknowledge the support from the Bioenergy Technologies Office of the U.S. Department of Energy under contract DE-AC02-06CH11357 for the Argonne National Laboratory. This work was authored in part by the National Laboratory of the Rockies, operated by Alliance for Sustainable Energy, LLC, for the U.S. Department of Energy (DOE) under contract no. DE-AC36-08GO28308. The advice from Tao Dong and Lieve Laurens from the National Renewable Energy Laboratory and Longwen Ou from the Argonne National Laboratory is also appreciated. The views and opinions of the authors expressed herein do not necessarily state or reflect those of the U.S. Government or any agency thereof or of any commercial entity. Neither the U.S. Government nor any agency thereof, nor any of their employees or employees of contributing companies, makes any warranty, expressed or implied, or assumes any legal liability or responsibility for the accuracy, completeness, or usefulness of any information, apparatus, product, or process disclosed or represents that its use would not infringe privately owned rights. The U.S. Government retains and the publisher, by accepting the article for publication, acknowledges that the U.S. Government retains a nonexclusive, paid-up, irrevocable, worldwide license to publish or reproduce the published form of this work, or allow others to do so, for U.S. Government purposes.

References

1 American Chemistry Council, Resin review 2023, *The Annual Statistical Report of the North American Plastics Industry*, Washington, D.C., United States, 2023.
2 *European Diisocyanate and Polyol Producers Association, What is polyurethane?*, https://www.polyurethanes.org/what-is-it/#:~:text=Polyurethaneisaplasticmaterial,cushioningforfurniture, accessed November 2, 2023.
3 D. B. Fishman, *New Foams Made Entirely from Algae Could Support Your Next Yoga Mat, Skateboard, or Mattress*, https://www.energy.gov/eere/bioenergy/articles/new-foams-made-entirely-algae-could-support-your-next-yoga-mat-skateboard, accessed November 2, 2023.
4 C. Liang, U. R. Gracida-Alvarez, E. T. Gallant, P. A. Gillis, Y. A. Marques, G. P. Abramo, T. R. Hawkins and J. B. Dunn, *Environ. Sci. Technol.*, 2021, **55**, 14215–14224.
5 American Chemistry Council, Sneak Peek: CPI Survey Unveils Positive Polyurethane Production Across North America. Polyurethane Production Increased in Key Sectors Between 2021-2023, *Helping Meet the Demand for Critical Products*, https://www.americanchemistry.com/chemistry-in-america/news-trends/press-release/2024/sneak-peek-cpi-survey-unveils-positive-polyurethane-production-across-north-america, accessed May 16, 2025.
6 A. Tenorio-Alfonso, M. C. Sánchez and J. M. Franco, *J. Polym. Environ.*, 2020, **28**, 749–774.
7 H. Lu, C. Dun, H. Jariwala, R. Wang, P. Cui, H. Zhang, Q. Dai, S. Yang and H. Zhang, *J. Controlled Release*, 2022, **350**, 748–760.

8 *Algenesis, Products*, https://www.algenesismaterials.com/algenesis-products, accessed January 8, 2024.
9 A. Cornille, R. Auvergne, O. Figovsky, B. Boutevin and S. Caillol, *Eur. Polym. J.*, 2017, **87**, 535–552.
10 C. Liang, Y. Jadidi, Y. Chen, U. Gracida-Alvarez, J. M. Torkelson, T. R. Hawkins and J. B. Dunn, *ACS Sustainable Chem. Eng.*, 2024, **12**, 12161–12170.
11 M. S. Kathalewar, P. B. Joshi, A. S. Sabnis and V. C. Malshe, *RSC Adv.*, 2013, **3**, 4110–4129.
12 T. Dong, E. Dheressa, M. Wiatrowski, A. P. Pereira, A. Zeller, L. M. L. Laurens and P. T. Pienkos, *ACS Sustainable Chem. Eng.*, 2021, **9**, 12858–12869.
13 M. Wiatrowski, B. C. Klein, R. W. Davis, C. Quiroz-Arita, E. C. D. Tan, R. W. Hunt and R. E. Davis, *Biotechnol. Biofuels Bioprod.*, 2022, **15**, 8.
14 L. Braud, K. McDonell and F. Murphy, *Renew. Sustain. Energy Rev.*, 2023, **179**, 113218.
15 P. Collet, A. Hélias, L. Lardon, J.-P. Steyer and O. Bernard, *Appl. Energy*, 2015, **154**, 1089–1102.
16 J. S. Castro, J. Ferreira, I. B. Magalhães, M. M. Jesus Junior, B. B. Marangon, A. S. A. P. Pereira, J. F. Lorentz, R. C. N. Gama, F. A. Rodrigues and M. L. Calijuri, *Renew. Sustain. Energy Rev.*, 2023, **187**, 113781.
17 R. M. Handler, C. E. Canter, T. N. Kalnes, F. S. Lupton, O. Kholiqov, D. R. Shonnard and P. Blowers, *Algal Res.*, 2012, **1**, 83–92.
18 A. T. Ubando, E. A. S. Ng, W.-H. Chen, A. B. Culaba and E. E. Kwon, *Bioresour. Technol.*, 2022, **360**, 127615.
19 M. Bussa, A. Eisen, C. Zollfrank and H. Röder, *J. Clean. Prod.*, 2019, **213**, 1299–1312.
20 R. Davis, T. R. Hawkins, A. Coleman, S. Gao, B. Klein, M. Wiatrowski, Y. Zhu, Y. Xu, L. Snowden-Swan, P. Valdez, J. Zhang, U. Singh and L. Ou, *Economic, Greenhouse Gas, and Resource Assessment for Fuel and Protein Production from Microalgae: 2022 Algae Harmonization Update*, National Renewable Energy Laboratory (NREL), Argonne National Laboratory (ANL), and Pacific Northwest National Laboratory (PNNL), Golden, CO, United States, 2024.
21 J. Zhang, Y. Zhu, T. R. Hawkins, B. C. Klein, A. M. Coleman, U. Singh, R. Davis, L. Ou, Y. Xu, S. Kar, M. Wiatrowski, S. Gao and P. Valdez, *Sustain. Energy Fuels*, 2025, **9**, 1859–1870.
22 H. Cai, L. Ou, M. Wang, R. Davis, M. Wiatrowski, A. Bartling, B. Klein, D. Hartley, P. Burli, Y. Lin, M. Roni, D. N. Thompson, L. Snowden-Swan, Y. Zhu, S. Li, Y. Xu and P. Valdez, *Supply Chain Sustainability Analysis of Renewable Hydrocarbon Fuels via Hydrothermal Liquefaction, Combined Algal Processing, and Biochemical Conversion: Update of the 2022 State-Of-Technology Cases*, Argonne National Laboratory, Lemont, IL, United States, 2023.
23 M. Wiatrowski, B. Klein, T. N. Do, L. Ou, H. Cai, N. Carlson and R. Davis, *Technology Case Study: Techno-Economic and Life Cycle Analysis for Microalgae Conversion Pathways to Fuels and Products*, National Renewable Energy Laboratory, Golden, CO, United States, 2025.
24 B. C. Klein, M. F. Chagas, R. E. Davis, M. D. B. Watanabe, M. R. Wiatrowski, E. R. Morais and L. M. L. Laurens, *Chem. Eng. J.*, 2024, **481**, 148462.
25 B. Ahn, S. Yun, S. Yun, Y.-J. Kim and W. Won, *Sustain. Prod. Consum.*, 2025, **55**, 340–352.
26 C. Dillon and M. Aguilera, New Science Behind Algae-based Flip-flops, https://today.ucsd.edu/story/new-science-behind-algae-based-flip-flops, accessed June 20, 2024.
27 Argonne National Laboratory, Greenhouse gases, Regulated Emissions, and Energy use in Technologies Model (GREET)® (2022 Excel), https://doi.org/10.2172/230197.
28 G.-J. Nabuurs, R. Mrabet, A. Abu Hatab, M. Bustamante, P. Clark, P. Havlik, J. House, C. Mbow, K. N. Ninan, A. Popp, S. Roe, B. Sohngen and S. Towprayoon, in *Climate Change 2022: Mitigation of Climate Change. Contribution of Working Group III to the Sixth Assessment Report of the Intergovernmental Panel on Climate Change*, Cambridge University Press, Cambridge, UK and New York, NY, USA, 1st edn., 2022.
29 M. A. J. Huijbregts, Z. J. N. Steinmann, P. M. F. Elshout, G. Stam, F. Verones, M. Vieira, M. Zijp, A. Hollander and R. van Zelm, *Int. J. Life Cycle Assess.*, 2017, **22**, 138–147.
30 P. Sun, A. Elgowainy, M. Wang, J. Han and R. J. Henderson, *Fuel*, 2018, **221**, 542–557.
31 R. Frischknecht, *Implementation of Life Cycle Impact Assessment Methods*, Swiss Centre for Life Cycle Inventories, Dubendorf, 2007.
32 B. Klein and R. Davis, *Algal Biomass Production via Open Pond Algae Farm Cultivation: 2022 State of Technology and Future Research*, National Renewable Energy Laboratory, Golden, CO, United States, 2023.
33 H. Cai, L. Ou, M. Wang, R. Davis, A. Dutta, K. Harris, M. Wiatrowski, E. Tan, A. Bartling, B. Klein, D. Hartley, Y. Lin, M. Roni, D. N. Thompson, L. Snowden-Swan and Y. Zhu, *Supply Chain Sustainability Analysis of Renewable Hydrocarbon Fuels via Indirect Liquefaction, Ex Situ Catalytic Fast Pyrolysis, Hydrothermal Liquefaction, Combined Algal Processing, and Biochemical Conversion: Update of the 2020 State-Of-Technology Cases*, Argonne National Laboratory, Lemont, IL, United States, 2021.
34 H. Cai, L. Ou, M. Wang, R. Davis, A. Dutta, K. Harris, M. Wiatrowski, E. Tan, A. Bartling, B. Klein, D. Hartley, P. Burli, Y. Lin, M. Roni, D. N. Thompson, L. Snowden-Swan, Y. Zhu and S. Li, *Supply Chain Sustainability Analysis of Renewable Hydrocarbon Fuels via Hydrothermal Liquefaction, Combined Algal Processing, and Biochemical Conversion: Update of the 2021 State-Of-Technology Cases*, Argonne National Laboratory, Lemont, IL, United States, 2022.
35 M. Wiatrowski and R. Davis, *Algal Biomass Conversion to Fuels via Combined Algae Processing (CAP): 2020 State of Technology and Future Research*, National Renewable Energy Laboratory, Golden, CO, United States, 2021.
36 H. Cai, J. Han, M. Wang, R. Davis, M. Biddy and E. Tan, *Biofuel Bioprod. Biorefining*, 2018, **12**, 815–833.
37 *ISO 14067, Greenhouse Gases — Carbon Footprint of Products — Requirements And Guidelines for Quantification*, International Organization for Standardiza, Switzerland, 2018.

38 R. Davis, J. Markham, C. Kinchin, N. Grundl, E. C. D. Tan and D. Humbird, *Process Design and Economics for the Production of Algal Biomass: Algal Biomass Production in Open Pond Systems and Processing through Dewatering for Downstream Conversion*, National Renewable Energy Laboratory, Golden, CO, United States, 2016.
39 J. G. S. -Hernández, F. I. G. -Castro, *Aspen Plus*, Aspen Technology, Inc., 2017.
40 M. Wiatrowski and R. Davis, *Algal Biomass Conversion to Fuels via Combined Algae Processing (CAP): 2022 State of Technology and Future Research*, National Renewable Energy Laboratory, Golden, CO, United States, 2023.
41 R. Davis and B. Klein, *Algal Biomass Production via Open Pond Algae Farm Cultivation: 2020 State of Technology and Future Research*, National Renewable Energy Laboratory, Golden, CO, United States, 2021.
42 U. Singh, S. Banerjee and T. R. Hawkins, *ACS Sustainable Chem. Eng.*, 2023, **11**, 14435–14444.
43 U. Lee, J. Han, M. Urgun Demirtas, M. Wang and L. Tao, *Lifecycle Analysis of Renewable Natural Gas and Hydrocarbon Fuels from Wastewater Treatment Plants' Sludge*, Argonne National Laboratory, Lemont, IL, United States, 2016.
44 R. Davis, C. Kinchin, J. Markham, E. C. D. Tan, L. M. L. Laurens, D. Sexton, D. Knorr, P. Schoen and J. Lukas, *Process Design and Economics for the Conversion of Algal Biomass to Biofuels: Algal Biomass Fractionation to Lipid- and Carbohydrate-Derived Fuel Products*, National Renewable Energy Laboratory, Golden, CO, United States, 2014.
45 A. W. Bartling, P. T. Benavides, S. D. Phillips, T. Hawkins, A. Singh, M. Wiatrowski, E. C. D. Tan, C. Kinchin, L. Ou, H. Cai, M. Biddy, L. Tao, A. Young, K. Brown, S. Li, Y. Zhu, L. J. Snowden-Swan, C. R. Mevawala and D. J. Gaspar, *ACS Sustainable Chem. Eng.*, 2022, **10**, 6699–6712.
46 U. Lee, A. Bhatt, T. R. Hawkins, L. Tao, P. T. Benavides and M. Wang, *J. Clean. Prod.*, 2021, **311**, 127653.
47 K. Lee, X. Liu, P. Vyawahare, P. Sun, A. Elgowainy and M. Wang, *Green Chem.*, 2022, **24**, 4830–4844.
48 R. Hasanzadeh, P. Mojaver, S. Khalilarya, T. Azdast, A. Chitsaz and M. Mojaver, *Polymers*, 2022, **14**, 4938.
49 *Trading economics, Naphtha*, https://tradingeconomics.com/commodity/naphtha, accessed May 16, 2023.
50 U.S. Energy Information Administration, U.S. No. 2 Diesel ultra Low sulfur less than 15 ppm retail sales by refiners, https://www.eia.gov/dnav/pet/hist/LeafHandler.ashx?n=pet&s=ema_epd2dxl0_ptg_nus_dpg&f=a, accessed May 16, 2023.
51 U.S. Bureau of labor statistics, Average energy prices for the United States, regions, census divisions, and selected metropolitan areas, https://data.bls.gov/pdq/SurveyOutputServlet, accessed May 16, 2023.
52 J. Zhang, F. Naaz, U. Singh, T. R. Hawkins, S. T. Crafton-Tempel, S. J. Edmunson, J. Caminiti, J. D. Watkins, P. J. Valdez and M. Huesemann, *npj Ocean Sustain.*, 2025, 47.
53 W. Zhang, T. Wang, Z. Zheng, R. L. Quirino, F. Xie, Y. Li and C. Zhang, *Chem. Eng. J.*, 2023, **452**, 138965.
54 ISOPA, REACH Restriction on diisocyanates, https://www.isopa.org/reach-restriction-on-diisocyanates/, accessed January 11, 2024.
55 National Center for Biotechnology Information, PubChem Compound Summary for CID 11443, Toluene 2,4-Diisocyanate., https://pubchem.ncbi.nlm.nih.gov/compound/Toluene-2_4-Diisocyanate, accessed November 4, 2025.
56 U.S. Environmental Protection Agency, Integrated Risk Information System (IRIS). 2,4-/2,6-Toluene diisocyanate mixture (TDI), https://iris.epa.gov/ChemicalLanding/&substance_nmbr=503, accessed November 4, 2025.
57 National Center for Biotechnology Information, PubChem Compound Summary for CID 16402, Hexamethylenediamine, https://pubchem.ncbi.nlm.nih.gov/compound/16402, accessed November 6, 2025.
58 B. Wang, S. Ma, X. Xu, Q. Li, T. Yu, S. Wang, S. Yan, Y. Liu and J. Zhu, *ACS Sustainable Chem. Eng.*, 2020, **8**, 11162–11170.
59 B. Quienne, F. Cuminet, J. Pinaud, M. Semsarilar, D. Cot, V. Ladmiral and S. Caillol, *ACS Sustainable Chem. Eng.*, 2022, **10**, 7041–7049.
60 A. Caschera, T. Calayan, N. Piccolo, A. Kakroodi, J. J. Robinson and G. Sacripante, *Polymers*, 2024, **16**, 2071.
61 A. Bukowczan, I. Łukaszewska and K. Pielichowski, *J. Therm. Anal. Calorim.*, 2024, **149**, 10885–10899.
62 International Textile Manufacturers Federation, Project 2: The Complete sets of technology development for bio-based polyamide 56 industrial chain, https://www.itmf.org/images/dl/awards/2022/Cathay-Biotech-Inc-with-Donghua-University.pdf, accessed December 19, 2023.
63 X. Wang, S. Gao, J. Wang, S. Xu, H. Li, K. Chen and P. Ouyang, *Chin. J. Chem. Eng.*, 2021, **30**, 4–13.
64 A. Manzardo, A. Marson, M. Roso, C. Boaretti, M. Modesti, A. Scipioni and A. Lorenzetti, *ACS Omega*, 2019, **4**, 14114–14123.
65 D. G. Kulas, M. C. Thies and D. R. Shonnard, *ACS Sustainable Chem. Eng.*, 2021, **9**, 5388–5395.
66 P. Quinteiro, N. V. Gama, A. Ferreira, A. C. Dias and A. Barros-Timmons, *J. Clean. Prod.*, 2022, **371**, 133554.